EMBO reports

scientific report

The structure of the TRAPP subunit TPC6 suggests a model for a TRAPP subcomplex

Daniel Kümmel[1,2], Jürgen J. Müller[1], Yvette Roske[1,3], Rolf Misselwitz[1], Konrad Büssow[3,4] & Udo Heinemann[1,2+]

[1]Max-Delbrück Center for Molecular Medicine, Berlin, Germany, [2]Chemistry Institute, Free University, Berlin, Germany, [3]Protein Structure Factory, Berlin, Germany, and [4]Max Planck Institute for Molecular Genetics, Berlin, Germany

The TRAPP (transport protein particle) complexes are tethering complexes that have an important role at the different steps of vesicle transport. Recently, the crystal structures of the TRAPP subunits SEDL and BET3 have been determined, and we present here the 1.7 Å crystal structure of human TPC6, a third TRAPP subunit. The protein adopts an α/β-plait topology and forms a dimer. In spite of low sequence similarity, the structure of TPC6 strikingly resembles that of BET3. The similarity is especially prominent at the dimerization interfaces of the proteins. This suggests heterodimerization of TPC6 and BET3, which is shown by *in vitro* and *in vivo* association studies. Together with TPC5, another TRAPP subunit, TPC6 and BET3 are supposed to constitute a family of paralogous proteins with closely similar three-dimensional structures but little sequence similarity among its members.

Keywords: BET3 protein family; Golgi membrane; TPC6 protein; TRAPP complex; vesicle tethering

EMBO reports advance online publication 15 July 2005;
doi:10.1038/sj.embor.7400463

INTRODUCTION

The intracellular transport of proteins and other molecules in vesicles is an essential process in eukaryotic cells. The TRAPP (transport protein particle) complexes are tethering complexes that have an important role in the recruitment of vesicles to the Golgi network. TRAPP I binds endoplasmic-reticulum-derived vesicles to the Golgi, whereas TRAPP II is involved in transport within the Golgi. Most TRAPP subunits are highly conserved between yeast and mammals (Barrowman *et al*, 2000; Sacher *et al*, 2001).

The recruitment of vesicles to the target membrane is mediated through the interaction of Rab-GTPases (Jahn *et al*, 2003) with effectors, such as the coiled-coil protein Uso1p, or tethering complexes, such as the exocyst and the COG (conserved oligomeric Golgi) complex, which have been classified as quadrefoil tethers (reviewed by Whyte & Munro, 2002). TRAPP does not belong to the quadrefoil complexes, but was shown to interact with COPII vesicles and promote nucleotide exchange of the Ypt1p Rab-GTPase (Sacher *et al*, 2001). The tethering process is followed by SNARE (soluble *N*-ethylmaleimide-sensitive factor attachment protein receptor)-mediated membrane fusion.

Immunoprecipitation and tandem affinity purification of the central subunit Bet3p allowed purification of the complete TRAPP complex and subsequent identification of other subunits (Sacher *et al*, 2001; Gavin *et al*, 2002). TRAPP I contains seven subunits in yeast (Bet3p, Bet5p, Trs20p, Trs23p, Trs31p, Trs33p and Trs85p) and TRAPP II, in addition, contains three subunits (Trs65p, Trs120p and Trs130p).

Two mammalian orthologues of yeast TRAPP subunits have been structurally characterized. The mouse SEDL protein (homologue Trs20p; Jang *et al*, 2002) is a monomeric (α + β) protein. The protein shares structural similarity with the amino-terminal regulatory domain of the SNAREs Ykt6p and Sec22b and is expected to be involved in many protein–protein interactions. Recently, the crystal structures of BET3 from the mouse (Kim *et al*, 2005) and human (Turnbull *et al*, 2005) have been published. BET3 was shown to form dimers and to be acylated at a conserved cysteine residue. It was shown that BET3 is membrane anchored; however, acylation seemed dispensable for this process. A hydrophobic tunnel that buries the covalently attached fatty acid moiety could alternatively accommodate fatty acids from an anchor protein, and a pattern of positively charged residues has been proposed to mediate membrane association of BET3 and, thus, the entire TRAPP complex.

TPC6, a human orthologue of yeast Trs33p, is encoded by a complementary DNA clone of the German cDNA consortium (Wellenreuther *et al*, 2004). We present here the structure of human TPC6 at 1.7 Å resolution. The protein shows an α/β-plait topology and forms a dimer in the crystal and in solution. Considering the conserved structures of TPC6 and BET3, we suggest a common fold for all paralogous BET3 family proteins, which include another TRAPP subunit, TPC5. Two common motifs had earlier been identified in these proteins, $LX_2\#GX_2\#GX_2LXE$ and $G\#_2XGXL$ (X represents any amino acid

[1]Max-Delbrück Center for Molecular Medicine, Robert-Rössle-Strasse 10, 13092 Berlin, Germany
[2]Chemistry Institute, Free University, Takustrasse 6, 14195 Berlin, Germany
[3]Protein Structure Factory, Heubnerweg 6, 14059 Berlin, Germany
[4]Max Planck Institute for Molecular Genetics, Ihnestrasse 73, 14195 Berlin, Germany
[+]Corresponding author. Tel: +49 30 9406 3420; Fax: +49 30 9406 2548;
E-mail: heinemann@mdc-berlin.de

Received 21 February 2005; revised 17 May 2005; accepted 25 May 2005; published online 15 July 2005

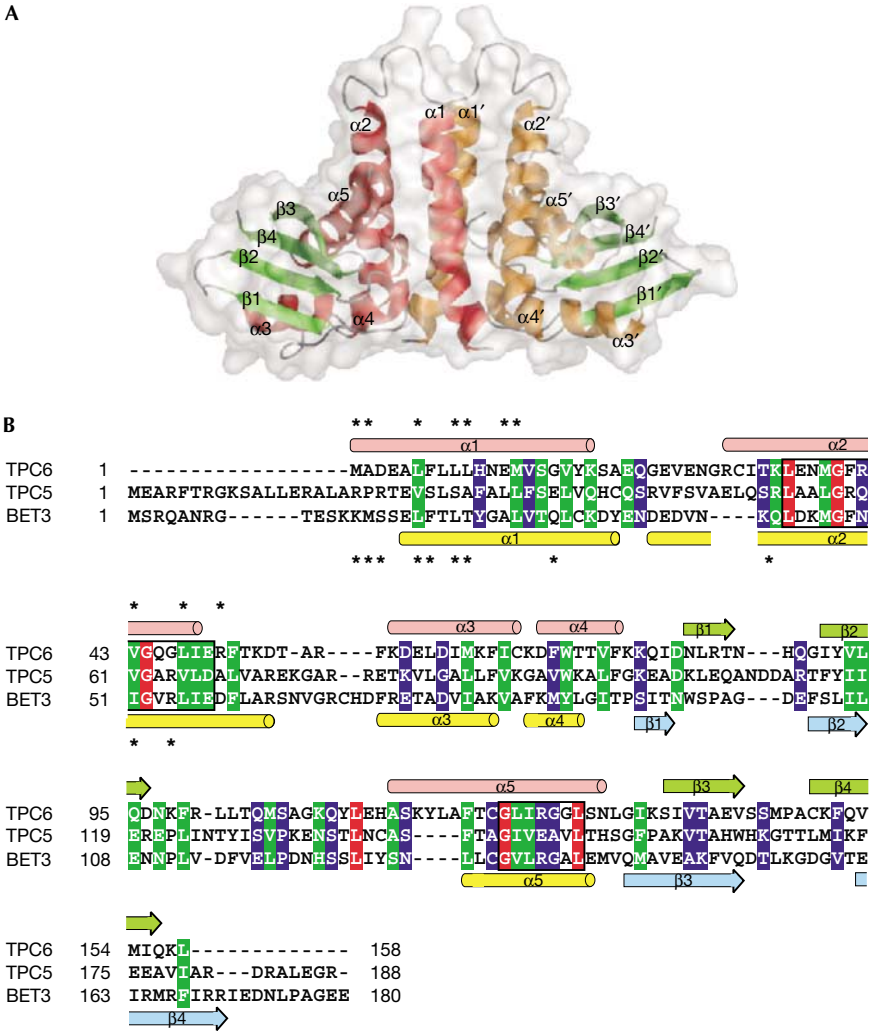

Fig 1 | Overall structure of TPC6. (**A**) Schematic representation of the TPC6 dimer with labelled helices (red and orange) and strands (green) on a semitransparent molecular surface. Unless stated otherwise, pictures were prepared using PyMOL (DeLano, 2003). (**B**) Multiple sequence alignment of human TPC6, TPC5 and BET3 (GenBank accession numbers AL833179, BC042161 and AF041432, respectively). The secondary structure elements of TPC6 and BET3 are represented above and below the aligned sequences. Identical, strongly similar and weakly similar residues are highlighted in red, green and blue, respectively. Residues of TPC6 and BET3 marked by an asterisk denote amino acids most strongly involved in dimer formation. Sequences corresponding to the BET3 family motif are enclosed in boxes. The multiple sequence alignment was prepared using CLUSTAL (Higgins *et al*, 1992).

and # a hydrophobic residue; Sacher *et al*, 2000). The similarity between TPC6 and BET3 is especially prominent at the dimerization interface of the proteins. This suggests heterodimerization of TPC6 and BET3, which we prove by *in vitro* and *in vivo* association studies. We therefore describe a first putative TRAPP subcomplex with important implications for the assembly of this tethering complex.

RESULTS AND DISCUSSION

Structure of TPC6

In the crystal, two TPC6 molecules are present per asymmetric unit, forming a dimer (Fig 1A). Each TPC6 subunit shows an α/β-plait topology, defining TPC6 as a member of the (α + β) class of proteins. Five α-helices are arranged on one side of a twisted, antiparallel, four-stranded β-sheet, and a 3_{10}-helix segment comprises the residues R100–L102. The arrangement of secondary structure elements with regard to the primary structure is shown in Fig 1B. Two carboxy-terminal residues and the loop 6 (T103–H114) are not visible in the electron-density map owing to disorder. The root-mean-square deviation (r.m.s.d.) between equivalent C^{α} atoms after a superposition of the two molecules per asymmetric unit with the program LSQKAB (Kabsch, 1976) is 0.5 Å. There are differences in the conformation of both monomers, mainly because of different crystal contacts of the chains. In addition, the loop region 2 (E51–E63) is partially disordered and missing in chain A. Considering the structural variability in these regions, depending on crystal contacts and a large number of disordered side chains, these areas have

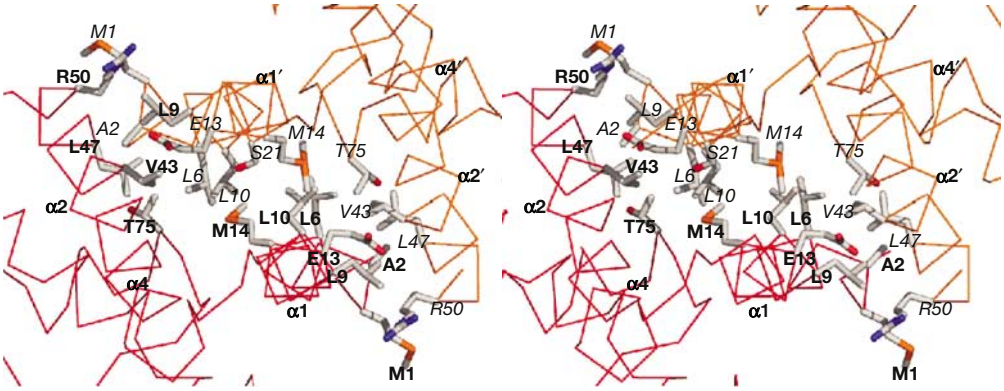

Fig 2 | Stereo image of the TPC6 interaction interface. For both monomers (coloured red and orange), the residues most strongly involved in dimerization are shown. Amino acids from different chains are labelled in bold print and italic font.

to be considered flexible in solution and might acquire order after TRAPP complex formation.

Between the helical face and the β-sheet of each chain, a wide depression is found (Fig 1A). This region might represent a binding surface for another TRAPP complex subunit. Dimerization of TPC6 occurs by means of the helical face of the protein, through the interaction of the helices α1 and α2 with α1′ and α2′, respectively, with minor contributions from α4 and α4′ (Fig 2). The surface area buried in the dimerization interface covers 2,396 Å^2, corresponding to 15.7% of the total solvent-accessible surface area (15,203 Å^2) of both monomers, as calculated with XSAE (courtesy Clemens Broger). The contact areas are mainly composed of hydrophobic and van der Waals interactions between aliphatic residues without any buried water molecules. The most prominent residues, with a contribution of >40 Å^2 to the dimerization interface, are M1, A2, L6, L9, L10, E13 and M14 (and S21 in chain A) in helix α1, V43, L47 and R50 in helix α2 and T75 in α4.

Structural comparison of TPC6 and BET3

The overall structure of TPC6 strikingly resembles that of BET3 (Fig 3A; Protein Data Bank entry 1SZ7 was used as a model for BET3). In spite of only 17% sequence identity, the superposition over 74% (TPC6 sequence) of the α-carbon backbones of the monomers of both proteins with LSQKAB (Kabsch, 1976) shows an r.m.s.d. of 1.5 Å. Differences in structure are mainly confined to the loop regions, whereas the α/β-plait cores of both proteins show little divergence.

A hydrophobic tunnel is located on the α-helical face of BET3. In the structure of human BET3 purified from yeast, it could be shown that a palmitic acid that is covalently bound to the conserved cysteine residue 68 occupies this cavity, whereas mouse BET3 purified from *Escherichia coli* was found to be acylated with a mixture of palmitate and myristate chains (Kim *et al*, 2005; Turnbull *et al*, 2005). No acylation is observed for TPC6, consistent with the absence of an equivalent cysteine. In TPC6, the area corresponding to the hydrophobic cavity of BET3 is entirely closed (Fig 3B), because there is less space between helices α3/α4 and α5 in TPC6. The remaining space is filled with hydrophobic residues, among which are four phenylalanines. TPC6 F58 is located at the position of the acylated residue C68 in BET3, thus blocking the channel entrance. The position of BET3 A82 is occupied by F72 in TPC6. It is interesting to note that the mutation A82L in BET3 led to a channel-blocking mutant that was no longer able to associate specifically with Golgi membranes (Kim *et al*, 2005). Finally, TPC6 F51, I64, F67 and L134 at the positions of BET3 F59, T74, V77 and V142 point into the centre of the cavity.

Another feature described for BET3 is a wide and flat dimer surface with a number of positively charged residues. Mutation of some of these basic residues resulted in a loss of BET3's capacity to associate with membranes (Kim *et al*, 2005). This suggests that the positively charged amino acids mediate membrane association, probably by interacting with the acidic head groups of phospholipids. For comparison of the corresponding faces of TPC6 and BET3, potential maps of both proteins were calculated (Fig 3C). TPC6 does not show the flat, positively charged surface strip described for BET3. The pattern of acidic and basic solvent-exposed amino acids yields a rather mixed charge distribution, and the surface is more uneven. The side chains of many of the charged residues of TPC6 in that region are flexible in the crystal, and TPC6 might be able to adjust to a negatively charged membrane. However, we suggest that TPC6, in contrast to BET3, is probably unable to promote membrane association of TRAPP. This is supported by our finding that in membrane preparations of cells expressing TPC6 and BET3, only BET3, but not TPC6, was found in microsomal fractions (supplementary Fig 7 online). The comparison of both proteins also shows a prominent conformational difference that can be observed at helix α2 (supplementary Fig 8 online), which supports the model for the extrusion of the covalently bound palmitate from BET3 (Turnbull *et al*, 2005).

A common fold for the BET3 protein family

Considering the high structural similarity between TPC6 and BET3, we suggest that the α/β-plait fold might represent the common fold for all paralogous BET3 family members. A sequence alignment of the human proteins TPC6, TPC5 and BET3 (Fig 1B) shows that conserved and similar residues between different family members are predominantly located in the α-helical secondary structure elements. Principal variations in length and conservation of the primary structure are only found in loop regions. In addition, the proteins differ in the length and

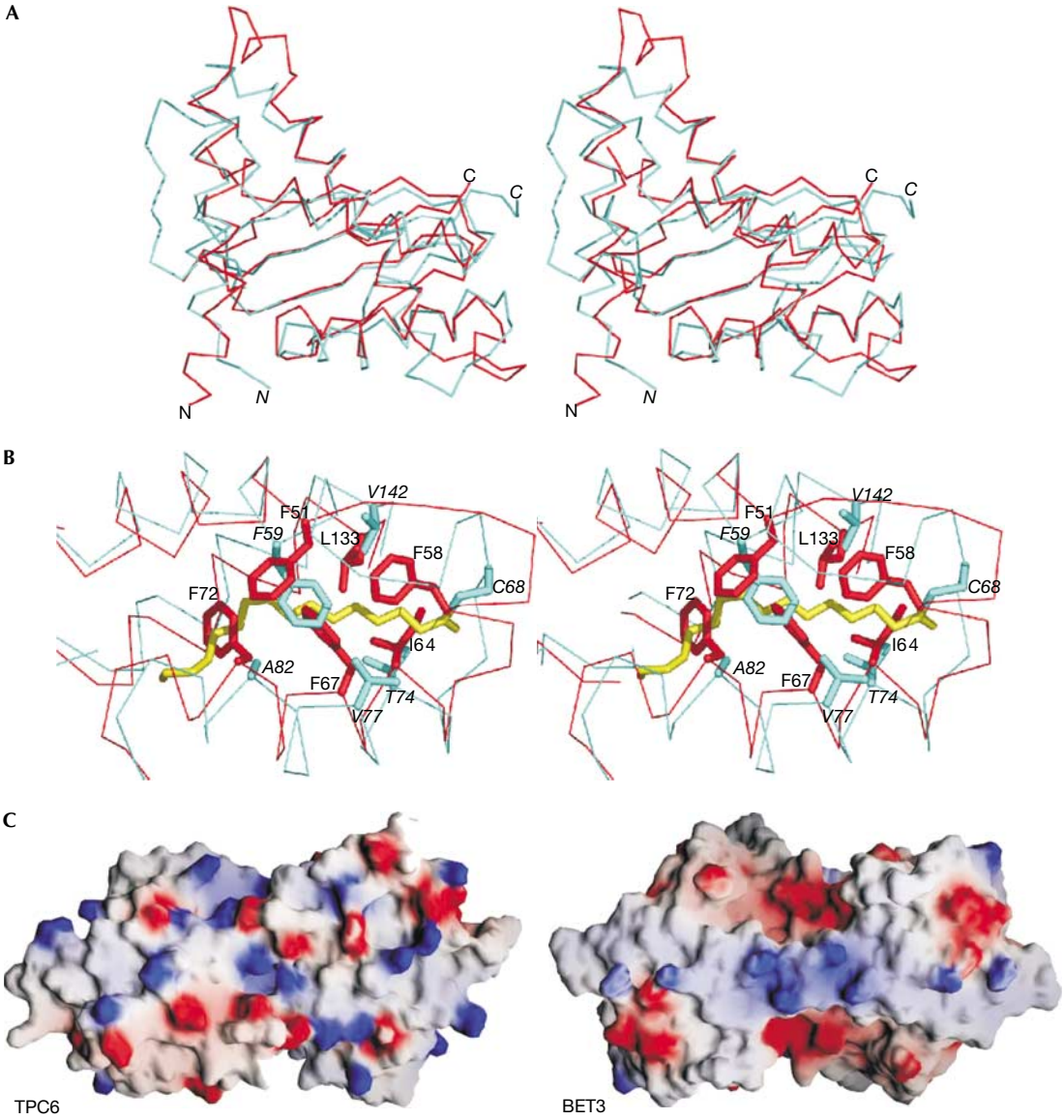

Fig 3 | Structural comparison of TPC6 (red) and BET3 (cyan). (**A**) Superposition of the TPC6 and BET3 monomers. (**B**) Placement of palmitate (yellow) from the hydrophobic cavity of BET3 into the corresponding area of TPC6 after least-squares superposition of the protein chains. Six bulky hydrophobic residues of TPC6 occupy the tunnel accommodating the palmitate in BET3. Residues at the corresponding positions of BET3 are labelled in italics. (**C**) Flat surfaces of the TPC6 and BET3 dimers. An electrostatic potential map calculated with DELPHI (Rocchia *et al*, 2001) is projected onto the molecular surface of the proteins using GRASP (Nicholls *et al*, 1991). Positive and negative potential are coloured blue and red, respectively, at the 10 kT level.

sequence of their N and C termini. The highest similarity is found for two motifs (LX_2#GX_2#GX_2LXE and G#$_2$XGXL) that have been previously described for the yeast BET3 family members (Sacher *et al*, 2001). These motifs are mostly conserved in the human proteins as well, and they are located in the interior of the proteins in helices α2 and α5. To test the hypothesis of a common family fold, the proteins have been purified and characterized by circular dichroism (CD) spectroscopy (Fig 4). The shapes of the CD spectra are similar, but show differences in their amplitudes. This can be explained with the different ratio of core region with similar secondary structure to unordered loop and terminal regions for TPC6 and BET3. Considering the primary structure of TPC5, which is similar to BET3 in the length of putative disordered regions, it is not surprising that its CD spectrum resembles the BET3 spectrum more than that of TPC6. CD spectroscopy and the sequence alignment, taken together, suggest that TPC5 may adopt a fold similar to that of TPC6 and BET3.

Interaction of TPC6 and BET3

In the crystal structure of TPC6, two molecules form a dimer with subunits related by a non-crystallographic dyad axis. The dimerization of BET3 occurs at a two-fold crystallographic axis.

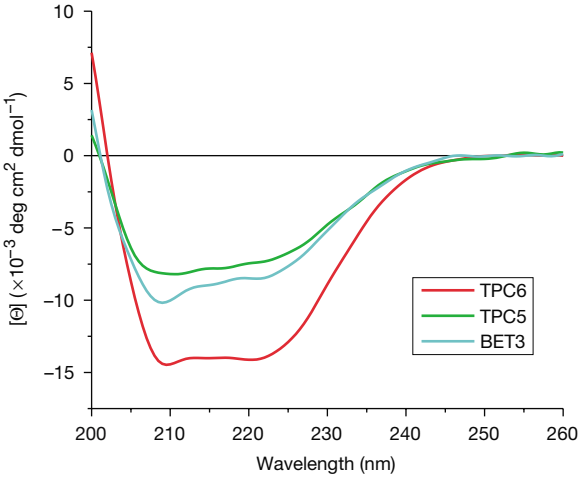

Fig 4 | Circular dichroism spectroscopy of BET3 family proteins. Spectra of recombinant TPC6, TPC5 and BET3 were recorded, as described.

Nevertheless, dimerization of both proteins occurs in a similar manner. The intermolecular interactions are mostly mediated by hydrophobic interactions of aliphatic residues located on the helices α1, α2 and, with less contribution, α4. The comparison of the important residues for dimerization of TPC6 and BET3 led to the identification of two similar sets of amino acids in helices α1 and α2, which are marked by asterisks in Fig 1B. The similarities in the dimerization surfaces of both proteins lead to the intriguing possibility of a heterodimerization between TPC6 and BET3.

A direct interaction between TPC6 and BET3 could be proven with association studies. In a pulldown of recombinant histidine (His)-tagged TPC6 with BET3 and TPC5 transiently expressed in human embryonic kidney (HEK) 293 cells, an interaction between TPC6 and BET3, but not between TPC6 and TPC5, was observed (Fig 5A). The TPC6–BET3 interaction can be shown *in vivo* by co-immunoprecipitation of Myc–BET3 with Flag–TPC6 (supplementary Fig 9 online).

To determine the intermolecular interactions between all BET3 protein family members, TPC6, BET3 and TPC5 were expressed in HEK 293 cells (Fig 5B). The immunoprecipitation of Myc–BET3 showed binding to both Flag–TPC6 and Flag–TPC5 individually. When all three proteins were expressed, there was no hindrance of TPC6 on the association of TPC5 with BET3, or vice versa.

The stoichiometry of the TPC6–BET3 interaction was determined by crosslinking experiments (Fig 5C). Homodimer formation of both proteins in solution was shown when they were crosslinked separately with glutaraldehyde. An equimolar mixture of TPC6 and BET3 led to the formation of heterodimers, which was confirmed by the identification of both proteins from the putative heterodimer band with mass spectrometry (not shown). The addition of TPC5 did not disturb TPC6–BET3 heterodimerization or the formation of TPC6 homodimers and BET3 homodimers, and no oligomerization of TPC5 and interaction with TPC6 or BET3 was observed under these conditions.

Our findings are at variance with earlier studies, which failed to show a direct interaction between the mouse Trs33 and BET3 (Kim *et al*, 2005). A direct interaction between BET3 and TPC5, as suggested by yeast two-hybrid analysis, could be detected *in vivo*, but not in our *in vitro* system. Post-translational modifications or a cofactor may be required to promote the interaction of TPC5 and BET3.

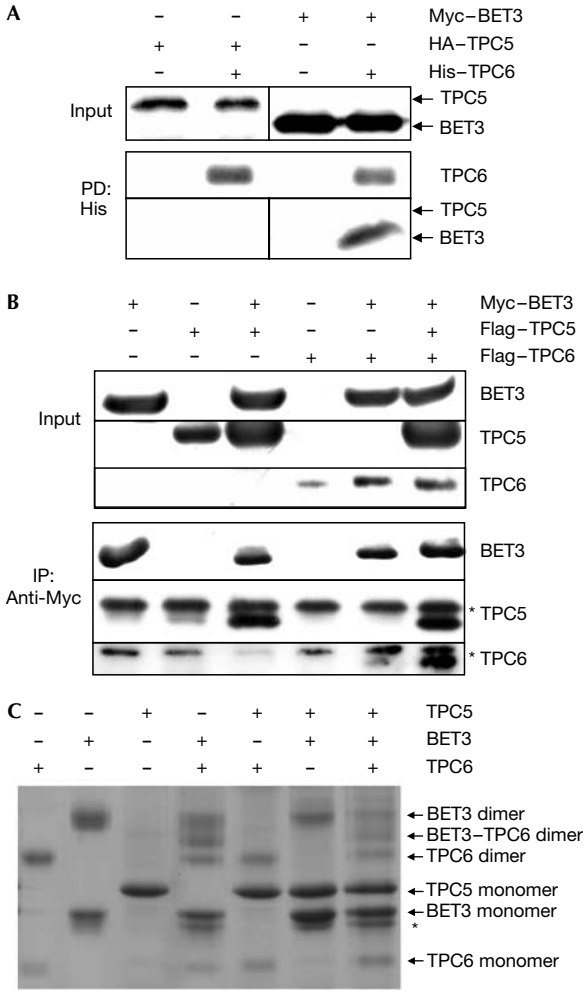

Fig 5 | Interactions between TPC6, BET3 and TPC5. (**A**) Histidine (His)-pulldown (PD) of recombinant 7 × His-tagged TPC6 with BET3 and TPC5 expressed in HEK 293 cells. Western blots were probed with anti-Myc and anti-HA antibodies and anti-His-HRP conjugate. (**B**) TPC6, BET3 and TPC5 were expressed in HEK 293 cells. The immunoprecipitation (IP) of Myc–BET3 led to the co-precipitation of Flag–TPC6 and Flag–TPC5. Western blots were probed with anti-Myc and anti-Flag antibodies. Unspecific Flag antibody bands are marked by asterisks. (**C**) Crosslinking of TPC6, BET3 and TPC5. Proteins alone and as mixtures were incubated with glutaraldehyde, as described. A BET3 degradation product is marked by an asterisk.

Speculation

We found that TPC6 and BET3 dimerize in a similar manner and are able to form heterodimers. We therefore suggest a model for a putative TRAPP subcomplex, in which TPC6 and BET3 form heterodimers using their similar dimer interfaces (Fig 6). As the TRAPP subunits are supposed to be present in equimolar stoichiometry in the TRAPP tethering complex, the assembly of the complex was thought to involve the association of dimeric BET3 and pairs of monomeric proteins such as SEDL (Turnbull

Fig 6 | Model of a TPC6–BET3 heterodimer. The structure of this TRAPP subcomplex is derived from a superposition of the TPC6 (red) and BET3 (cyan) dimers.

Table 1 | Refinement statistics

Resolution (Å)	23–1.7
R_{work}[a] (%)	17.5
R_{free}[b] (%)	20.9
R.m.s.d. bond distances (Å)	0.018
R.m.s.d. bond angles (deg)	1.74
Mean *B*-value (Å^2)	31.5
Ramachandran plot[c] (%)	
Most favoured	92.2
Additionally allowed	7.8
Generously allowed	0.0
Disallowed	0.0

[a]$R_{work} = \sum||F(obs)|-|F(calc)||/\sum F(obs)|$ for the 95% of the reflection data used in refinement.
[b]$R_{free} = \sum||F(obs)|-|F(calc)||/\sum F(obs)|$ for the remaining 5%.
[c]According to PROCHECK (Laskowski *et al*, 1993).

et al, 2005). Our results open up the alternative possibility that a TPC6–BET3 heterodimer represents a TRAPP subcomplex *in vivo* and functions as a starting point for complex assembly at the Golgi membrane. According to this model, all TRAPP subunits could be present with one copy, in fair agreement with a molecular mass of ~300 kDa as reported for TRAPP I (Sacher *et al*, 2001). We suggest that other TRAPP proteins associate with specific binding pockets on BET3 and TPC6, which subsequently may lead to the formation of the complete TRAPP complex.

METHODS

Protein expression and purification. The human *TPC6* and *TPC5* cDNAs were cloned into the bacterial expression vector pQTEV (Scheich *et al*, 2004) and expressed in superior broth (SB) medium with 1 mM isopropyl-1-thio-β-D-galactopyranoside.

TPC6 was purified with Ni affinity chromatography, after tag cleavage by the tobacco etch virus (TEV) protease (encoding plasmid was kindly provided by Gunter Stier, EMBL Heidelberg). TPC6 was subjected to size-exclusion chromatography and concentrated to 9.7 mg ml^{-1}. TPC5 was purified from inclusion bodies under denaturing conditions (8 M urea) and refolded on a column with a 90 min gradient from 6 to 1 M urea. After dialysis against phosphate-buffered saline (PBS), folding of the protein was confirmed with CD spectroscopy. Selenomethionine-labelled TPC6 was produced according to the protocol of Budisa *et al* (1995). BET3 was expressed and purified essentially, as described previously (Turnbull *et al*, 2005). Detailed cloning and purification procedures are available as the supplementary information online.

Crystallization and data collection. TPC6 crystals were obtained at 20 °C by the sitting-drop method using a semi-automated dispensing system (Mueller *et al*, 2001). The best crystals (space group *C*2) were obtained in 22–23% PEG 3350, 0.1 M HEPES pH 7.5 and 0.3 M $(NH_4)_2SO_4$ or 0.4 M Li_2SO_4.

Data from a native crystal to 1.7 Å and a derivative crystal to 1.9 Å resolution were collected at 100 K at the Protein Structure Factory beamlines BL1 and BL2 of the Free University of Berlin at BESSY (Berlin, Germany). Data were reduced and scaled using HKL2000 (Otwinowski & Minor, 1997). Data collection statistics are listed in supplementary Table 2 online.

Structure determination. For structure determination of TPC6, selenium peak wavelength data to 2.4 Å resolution were used for single-wavelength anomalous diffraction phasing. Initial phases were calculated using SOLVE (Terwilliger & Berendzen, 1999), and density modification, implemented in RESOLVE (Terwilliger, 2000), was used to improve phases. The initial model comprising 58% of 320 residues per asymmetric unit was automatically built with RESOLVE and interactively improved using the program O (Jones *et al*, 1991). The model was placed into the isomorphous unit cell of the high-resolution native protein data and subsequently refined using REFMAC5 (Murshudov *et al*, 1997). During several rounds of iterative model building and refinement (including TLS), the model was extended to 290 residues per asymmetric unit, and five sulphate ions, four glycerol and 126 water molecules were placed in the electron density map. The coordinates and diffraction amplitudes were deposited in the Protein Data Bank with accession code 2BJN. Refinement statistics are summarized in Table 1.

Association studies. His-pulldowns were performed with Talon resin (BD Bioscience, Heidelberg, Germany) preincubated with recombinant TPC6 and lysates from HEK 293 cells transiently expressing BET3 and TPC5. Immunoprecipitations were performed with Myc–BET3, Flag–TPC5 and Flag–TPC6 transiently expressed in HEK 293 cells and analysed by SDS–polyacrylamide gel electrophoresis (SDS–PAGE) and western blotting. Cross-linking experiments were performed with 0.1 mM glutaraldehyde for 2 h after preincubation of protein mixtures overnight. Samples were analysed by SDS–PAGE and Coomassie staining. For protein identification, bands were excised and subjected to in-gel trypsin digestion and liquid chromatography mass spectrometry (LC/MS-ESI). Detailed protocols are described in the supplementary information online.

Circular dichroism. For CD spectroscopy, protein samples were diluted to 0.1–0.05 mg ml^{-1} and dialysed against PBS. Measurements were carried out with a Jasco J720 spectropolarimeter at 20 °C from 260 to 200 nm at 0.1 cm pathlength. Protein concentrations were determined according to absorbance at 280 nm and molar mean residue ellipticities were calculated.

Supplementary information is available at *EMBO reports* online (http://www.emboreports.org).

ACKNOWLEDGEMENTS
We thank S. Kaminski and K. Behling for technical assistance, A. Turnbull and the staff at BESSY for beamline support, E.-C. Müller for mass spectrometry analysis and A. Oeckinghaus for help with the cell-culture experiments. This work was supported by the German Federal Ministry of Education and Research (BMBF) through the 'Leitprojektverbund Proteinstrukturfabrik', the National Genome Network (NGFN; FZK 01GR0471, 01GR0472) and by the Fonds der Chemischen Industrie.

REFERENCES
Barrowman J, Sacher M, Ferro-Novick S (2000) TRAPP stably associates with the Golgi and is required for vesicle docking. *EMBO J* **19:** 862–869
Budisa N, Steipe B, Demange P, Eckerskorn C, Kellermann J, Huber R (1995) High-level biosynthetic substitution of methionine in proteins by its analogs 2-aminohexanoic acid, selenomethionine, telluromethionine and ethionine in *Escherichia coli*. *Eur J Biochem* **230:** 788–796
DeLano WL (2003) *The PyMOL Molecular Graphics System*. DeLano Scientific LLC, San Carlos, CA, USA
Gavin AC *et al* (2002) Functional organization of the yeast proteome by systematic analysis of protein complexes. *Nature* **415:** 141–147
Higgins DG, Bleasby AJ, Fuchs R (1992) CLUSTAL V: improved software for multiple sequence alignment. *Comput Appl Biosci* **8:** 189–191
Jahn R, Lang T, Südhof TC (2003) Membrane fusion. *Cell* **112:** 519–533
Jang SB, Kim Y-G, Cho Y-S, Suh P-G, Kim K-H, Oh B-H (2002) Crystal structure of SEDL and its implications for a genetic disease spondyloepiphyseal dysplasia tarda. *J Biol Chem* **277:** 49863–49869
Jones TA, Zou JY, Cowan SW, Kjeldgaard M (1991) Improved methods for building protein models in electron density maps and the location of errors in these models. *Acta Crystallogr A* **47:** 110–119
Kabsch W (1976) A solution for the best rotation to relate two sets of vectors. *Acta Crystallogr A* **32:** 922–923
Kim YG, Sohn EJ, Seo J, Lee KJ, Lee HS, Hwang I, Whiteway M, Sacher M, Oh BH (2005) Crystal structure of bet3 reveals a novel mechanism for Golgi localization of tethering factor TRAPP. *Nat Struct Mol Biol* **12:** 38–45
Laskowski RA, MacArthur MW, Moss DS, Thornton JM (1993) PROCHECK: a program to check the stereochemical quality of protein structures. *J Appl Crystallogr* **26:** 283–291
Mueller U, Nyarsik L, Horn M, Rauth H, Przewieslik T, Saenger W, Lehrach H, Eickhoff H (2001) Development of a technology for automation and miniaturisation of protein crystallisation. *J Biotechnol* **285:** 7–14
Murshudov GN, Vagin AA, Dodson EJ (1997) Refinement of macromolecular structures by the maximum-likelihood method. *Acta Crystallogr D* **53:** 240–255
Nicholls A, Sharp KA, Honig B (1991) Protein folding and association: insights from the interfacial and thermodynamic properties of hydrocarbons. *Proteins Struct Funct Genet* **11:** 281–296
Otwinowski Z, Minor W (1997) Processing of X-ray diffraction data collected in oscillation mode. *Methods Enzymol* **276:** 307–326
Rocchia W, Alexov E, Honig B (2001) Extending the applicability of the nonlinear Poisson–Boltzmann equation: multiple dielectric constants and multivalent ions. *J Phys Chem B* **105:** 6507–6514
Sacher M, Barrowman J, Schieltz D, Yates III JR, Ferro-Novick S (2000) Identification and characterization of five new subunits of TRAPP. *Eur J Cell Biol* **79:** 71–80
Sacher M, Barrowman J, Wang W, Horecka J, Zhang Y, Pypaert M, Ferro-Novick S (2001) TRAPP I implicated in the specificity of tethering in ER-to-Golgi transport. *Mol Cell* **7:** 433–442
Scheich C, Niesen FH, Seckler R, Büssow K (2004) An automated *in vitro* protein folding screen applied to human dynactin subunit. *Protein Sci* **13:** 370–380
Terwilliger TC (2000) Maximum-likelihood density modification. *Acta Crystallogr D* **56:** 965–972
Terwilliger TC, Berendzen J (1999) Automated MAD and MIR structure solution. *Acta Crystallogr D* **55:** 849–861
Turnbull AP *et al* (2005) Structure of palmitoylated BET3: insights into TRAPP complex assembly and membrane localization. *EMBO J* **24:** 875–884
Wellenreuther R, Schupp I, The German cDNA Consortium, Poustka A, Wiemann S (2004) SMART amplification combined with cDNA size fractionation in order to obtain large full-length clones. *BMC Genom* **5:** 36
Whyte JR, Munro S (2002) Vesicle membrane complexes in membrane traffic. *J Cell Sci* **115:** 2627–2637